

Pressure-Induced Polymerization of Acrylic Acid: A Raman Spectroscopic Study

Chitra Murli[†] and Yang Song*

Department of Chemistry, The University of Western Ontario, London, Ontario N6A 5B7, Canada

Received: April 18, 2010; Revised Manuscript Received: June 23, 2010

We report here the first in-situ Raman spectroscopic study of pressure-induced structural and polymeric transformations of acrylic acid. Two crystalline phases (I and II) were observed upon compression to ~ 0.3 and ~ 2.7 GPa. Phase I can be characterized with a single *s-cis* molecular conformation with possibly a similar structure to the low-temperature phase, while phase II suggests significantly enhanced molecular interactions toward polymerization and structural disordering. Beyond ~ 8 GPa, spectroscopic features indicate the onset of polymerization. The high-pressure polymeric phase together with the pressure-quenched materials was examined and compared with two commercial acrylic acid polymers using Raman spectroscopy. The characteristics of polymeric acrylic acid and their transformation mechanisms as well as the implications of hydrogen-bonding interactions are discussed.

1. Introduction

Pressure-induced polymerization is a chemical process pertaining to green chemistry as the reactions can be carried out in the absence of any solvent or catalyst, which implies a lesser environmental impact. The application of pressure was found to have a significant impact on the addition-type polymerization in both liquid- and gas-phase systems because the transition state of an addition reaction occupies a smaller volume than the initial state.¹ As intermolecular interactions can be significantly tuned under pressure, monomers may undergo structural transitions to phases that are more favorable for polymerization via new reaction pathways producing novel properties that are distinct from those obtained using conventional synthetic methods.² The earliest pressure-induced polymerization studies of several simple monomers such as acrylamide, *p*-phenylstyrene, potassium *p*-styrenesulphonate, and so forth have been reported by Bradbury et al.³ More recently, Bini and co-workers have reported pressure-induced polymerization of ethylene, butadiene, phenoxy ethyl acrylate, isoprene, acetylene, propene, and so forth using pressure and optical “catalysis”.^{2,4–10} The nature of pressure-induced polymeric forms was found to depend upon the applied pressure, the transition kinetics, and the additional optical excitations. In the case of butadiene, for instance, pressure-induced dimerization was found to occur at pressures above 0.7 GPa. However, dimerization was completely suppressed by the rapid formation of pure *trans* polybutadiene upon irradiating the high-pressure sample with a few milliwatts of a 488 nm Ar⁺ laser.⁵ Similarly, ethylene transformed to low-density polyethylene when compressed above 3 GPa in the solid phase, whereas liquid ethylene was found to polymerize at 0.5 GPa under laser irradiation to form a high-density crystalline polymer.² These examples demonstrate that pressure-induced polymerization reactions with the aid of photon activation result in the reduction of the transition pressures and thus can be utilized for high-pressure synthesis with a possible extension to large volume applications.¹⁰

Poly(acrylic acid) is a well-known polymer with a wide variety of industrial applications such as being superabsorbent materials, biocompatible polymers in bioadhesive drug delivery systems, polyelectrolytes in electrochemical devices, and nanoparticles in molecular devices. The molecular weight as well as the conformational state of the polymer significantly influences its functionality and different potential applications. In addition, hydrogen-bonding interactions play an important role in tuning the structures and the functionalities of these polymeric systems. Acrylic acid (CH₂=CH–COOH), the monomer of poly(acrylic acid), exhibits unusual features in polymerization as it has a carboxyl group which readily undergoes molecular associations through hydrogen bonds. As hydrogen-bonding interactions have proven to be sensitive to compression,¹¹ studying the effect of pressure on structural transformations of acrylic acid would be of fundamental interest. Moreover, it is of great significance in the polymer industry to explore pressure-induced polymerization from this monomer as the polymer product with improved properties distinct from that obtained using conventional synthetic methods might be obtained.¹² We have therefore carried out in-situ high-pressure Raman investigations of this compound up to 10 GPa and here report the interesting structural transitions leading to the polymerization of acrylic acid.

2. Structural Details

Acrylic acid is the simplest unsaturated aliphatic acid. The molecular structures of the monomer and the dimer of acrylic acid have been extensively investigated by electron diffractions,¹³ vibrational spectroscopy,^{14–16} and ab initio calculations.¹⁶ Depending on the physical state, many conformers have been observed, of which the three most representative, that is, *s-cis*, *s-trans* (C–O), and *s-trans*, are shown in Figure 1a. For example, in argon and krypton matrixes, the acrylic acid monomer exists as a mixture of two conformers with similar energies differing only in the relative orientation of the C=C–C=O axis.¹⁶ Upon irradiation by a xenon lamp at $\lambda = 243$ nm, the *s-cis* conformer (with a C=C–C=O dihedral of 0°) corresponding to the conformational ground state converts to the *s-trans* conformer (with a C=C–C=O dihedral of 180°). In the liquid phase, dimeric structures strongly predominate, and both conformations

* To whom correspondence should be addressed. E-mail: yang.song@uwo.ca. Phone: 519-661-2111 ext 86310. Fax: 519-661-3022.

[†] Permanent address: High Pressure & Synchrotron Physics Division, Bhabha Atomic Research Centre, Mumbai, India 400085.

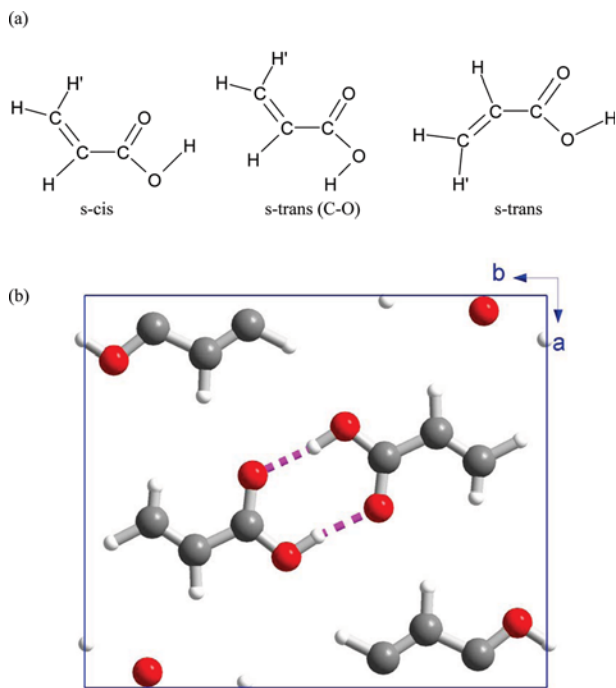


Figure 1. Molecular (a) and crystal (b) structures of acrylic acid. Three representative conformations (i.e., s-cis, s-trans (C–O), and s-trans) in liquid phase are adopted from ref 16. The crystal lattice is viewed along the *c*-axis, and only one layer of unit cell content on the *z* = 0 plane is depicted. The black, red, and white balls denote C, O, and H atoms, respectively. The hydrogen-bond interaction between two adjacent acrylic acid molecules is indicated by pink dashed lines.

were indicated by the vibrational spectra.¹⁶ In the solid phase, the structure of crystalline acrylic acid has been determined at 138 K using X-ray diffraction methods by Higgs and Sass.¹⁷ It belongs to an orthorhombic space group *I*bam (D_{2h}^{26}) with eight molecules per unit cell (or four molecules per primitive cell) with unit cell constants of $a = 9.966 \pm 0.007$ Å, $b = 11.744 \pm 0.013$ Å, and $c = 6.306 \pm 0.016$ Å. The molecules are planar hydrogen-bonded dimers lying on crystallographic mirror planes as shown in Figure 1b. From this perspective, Krause et al. have interpreted the vibrational spectra of acrylic acid on the basis of a primitive cell composed of two weakly interacting dimer molecules or four monomer molecules, whose modes are highly perturbed by hydrogen bonding to the nearest neighbor molecules.¹⁵

3. Experimental Section

High-purity (99%) acrylic acid monomer in the liquid form was purchased from Aldrich and was used without further purification. A symmetric diamond anvil cell equipped with a pair of type I diamonds with a culet size of 400 μm was used in the experiment. The liquid samples of acrylic acid were loaded into a hole with a diameter of 150 μm drilled on a stainless steel gasket that was preindented to a thickness of 90 μm. The pressure was determined using the well-established ruby fluorescence line with an uncertainty of ± 0.05 GPa under quasi-hydrostatic conditions.¹⁸ Raman measurements were carried out with a customized Raman microspectroscopy system. The 488 nm line of an Innova Ar⁺ laser from Coherent Inc. was used as the excitation source. The laser was focused to less than 5 μm on the sample with an average power of 30 mW by an Olympus microscope with a 20× objective. A 15× eyepiece and a digital camera allowed for the precise alignment of the focused laser beam on the sample. The Raman scattering

signal was collected by the same objective lens with a backscattering geometry. The Rayleigh scattering was removed by a pair of notch filters which enabled a measurable spectral range above 150 cm⁻¹. The scattered photons were focused on the entrance slit of a spectrometer and then were dispersed by an imaging spectrograph housing a monochromator with a 0.5 m focal length and equipped with multiple gratings. In this experiment, an 1800 lines/mm grating with 0.1 cm⁻¹ resolution was used. The Raman signal was recorded by an ultrasensitive liquid-nitrogen-cooled back-illuminated charge-coupled device (CCD) detector from Acton. The system was calibrated using neon lines with an uncertainty of ± 1 cm⁻¹. All measurements were conducted at room temperature.

4. Results and Discussion

We have carried out high-pressure investigations in two different sets of experiments in the lower pressure region of 0–4.5 GPa and in the higher pressure region of 3–10 GPa, respectively. In the lower pressure region, the maximum pressure was kept at ~ 4.5 GPa for hundreds of hours with an aim to examine qualitatively any possible kinetics involved in the pressure-induced structural transformations. In the higher pressure region, Raman spectra were collected both on compression and on decompression to examine the reversibility of the pressure-induced transformations.

A. Raman Spectra in the Pressure Region of 0–4.5 GPa.

The Raman spectrum of liquid acrylic acid at ambient condition is shown in Figure 2a. The Raman shifts observed in this study are listed in Table 1 in comparison with earlier studies.^{13–15} In general, the frequencies of most of the characteristic modes observed in this study agree very well with those reported previously, and thus their assignments can be obtained consistently from the earlier studies. However, the assignments of some modes, such as the $\nu(\text{CO}_2)_s$ symmetric stretch and the $\delta(\text{CH}_2)$ bending modes, are controversial.^{14,16} As the C–O bond length was found to reduce upon dimerization,¹³ the mode observed at 1433 cm⁻¹, which stiffens under pressure (see discussions below), is more likely to be the $\nu(\text{CO}_2)_s$ symmetric stretching mode. In contrast, the pressure-induced softening of the mode at 1393 cm⁻¹ (also see following sections) suggests that it might be associated with the $\delta(\text{CH}_2)$ bending mode. These assignments were suggested by Kulbida et al.¹⁶ and were adopted in Table 1 accordingly.

From Figure 2b, the Raman spectrum of acrylic acid indicates a liquid-to-solid transition at 0.3 GPa to a high-pressure crystalline phase (labeled as phase I) evidenced by the emergence of vibrational modes in the lattice region 100–200 cm⁻¹. In addition, the much sharper Raman band profile accompanied by the dramatic change of all the vibrational modes of the CO₂ group, including $\Omega(\text{CO}_2)$, $\omega(\text{CO}_2)$, $\nu(\text{CO}_2)_s$, and $\nu(\text{CO}_2)_{\text{asy}}$, together with the merging of the doublet $\delta(\text{C}=\text{C}-\text{C})$, $\delta(\text{O}=\text{C}-\text{O})$, and $\omega(\text{CH}_2)$ modes indicated significant changes in the molecular structures and conformations. These observations with the detailed vibrational frequencies are consistent with the previous low-temperature (i.e., 263 K) and ambient-pressure Raman measurements of solid acrylic acid (see Table 1) indicating that phase I was likely associated with a single s-cis molecular conformation with significant dimeric molecular interactions. Furthermore, such a liquid-to-solid transformation was most evident in the visual observation of the crystallization under an optical microscope (Figure 2 inset).

Figure 3 depicts the Raman spectra of acrylic acid at selected pressures between 0.3 and 4.5 GPa upon compression. The Raman profile displayed a smooth pressure evolution for all of

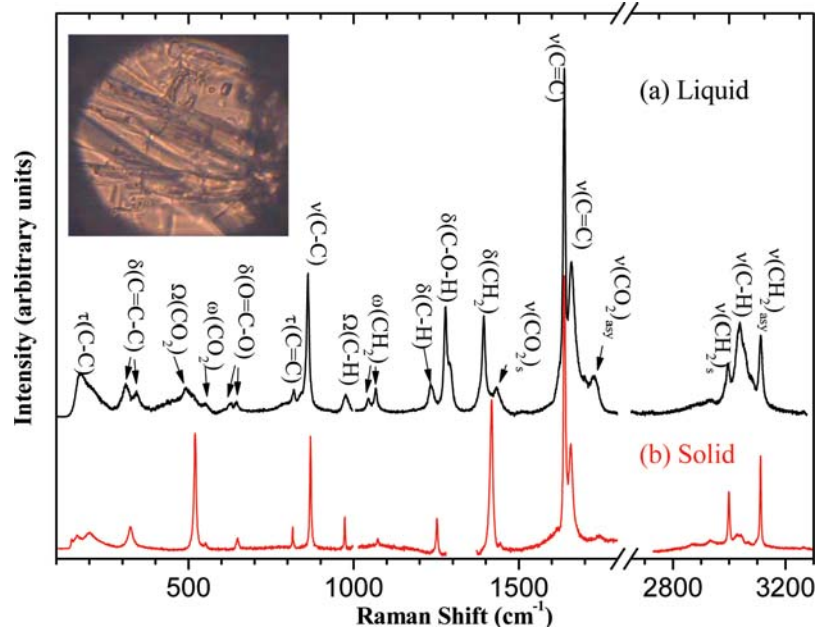


Figure 2. Room-temperature Raman spectrum of acrylic acid collected (a) at ambient pressure as a liquid and (b) at 0.3 GPa as a solid in the spectral region 100–3250 cm^{-1} . The spectral region of 1800–2700 cm^{-1} was truncated because of the lack of spectroscopic features. The assignments of the characteristic Raman modes are labeled for the liquid phase (see Table 1). The inset shows the photograph of acrylic acid upon crystallization at 0.3 GPa collected via an optical microscope.

TABLE 1: Observed Frequencies (cm^{-1}) of Raman Active Modes of Acrylic Acid with Assignments and Their Pressure Dependence, $d\nu/dP$ ($\text{cm}^{-1}/\text{GPa}$)

description ^a	this work					reference		
	liquid ν	solid ^b		solid ^c		liquid ^d ν	liquid ^e ν	solid ^f ν
$\nu(\text{CH}_2)_{\text{as}}$	3112	3111	8.8	3134	9.1	3112	3110	3108
$\nu(\text{C-H})$	3041	3035	5.8	3055	7.2	3039	3040	3041
$\nu(\text{CH}_2)_s$	2994	2999	7.1	3019	7.8	2998	2996	2996
$\nu(\text{CO}_2)_{\text{asy}}$	1726	1743				1728	1725/1705	1721
$\nu(\text{C=C})$	1660	1657	4.4	1669	1.0	1660	1658/1620	1657
	1638	1640	1.5	1644	1.1	1637	1636	1637
$\nu(\text{CO}_2)_s$	1433	1445		1444	4.2	1434	1430/1408	1444
$\delta(\text{CH}_2)$	1393	1417	5.9	1426	-3.1	1395	1396	1414
$\delta(\text{C-O-H})$	1280					1280	1280	1292/1283
$\delta(\text{C-H})$	1233	1252	7.4	1274	4.5	1232	1236	1252
				1260	5.0			
$\omega(\text{CH}_2)$	1067	1073	5.0	1086	4.0	1069	1068/1044	1073
	1045			1082	1.9	1048		
$\Omega(\text{C-H})$	976	973	3.7	986	4.1	977	997/926	973
				975	0.7			
$\nu(\text{C-C})$	850	869	6.1	887	4.7	861	861	867
$\tau(\text{C=C})$	818	816	0.0	816	0.5	820	818	818
$\delta(\text{O=C-O})$	645	649	3.2	659	3.3	643	642/628	642
	626			653	2.3	625		
$\omega(\text{CO}_2)$	552					548	525/548	535
$\Omega(\text{CO}_2)$	498	520	4.7	531	2.0	512	517	516
$\delta(\text{C=C-C})$	310	324	4.7	336	3.6	309	306/337	318
$\tau(\text{C-C})$	172	202	16.8	253	20.0			139
lattice modes		161	9.0	185	3.9			
		147	5.4	163	5.8			
				128	7.7			
				107	8.0			

^a Reference 16. ν : stretching; δ : bending; ω : wagging; Ω : out-of-plane; τ : torsion; s: symmetric; asy: asymmetric. ^b Frequencies were measured at 0.3 GPa and 300 K; $d\nu/dP$'s were measured in the pressure region of 0.3–2.7 GPa. ^c Frequencies were measured at 2.7 GPa and 300 K; $d\nu/dP$'s were measured in the pressure region of 2.7–8.0 GPa. ^d Reference 14. ^e Reference 16. Frequencies separated by a slash refer to those associated with s-cis/s-trans isomers (see Figure 1a). ^f Reference 16. Measured at 263 K and ambient pressure.

the characteristic vibrational modes except that obvious splittings were observed for $\delta(\text{O=C-O})$, $\Omega(\text{C-H})$, and $\omega(\text{CH}_2)$ modes above ~ 2.7 GPa indicating the formation of a new phase. The frequencies of the observed Raman modes as a function of

pressure are shown in Figure 4 with the corresponding pressure dependence (i.e., $d\nu/dP$ values) listed in Table 1. The different pressure dependence of most of the characteristic modes and the appearance of new modes because of splitting also col-

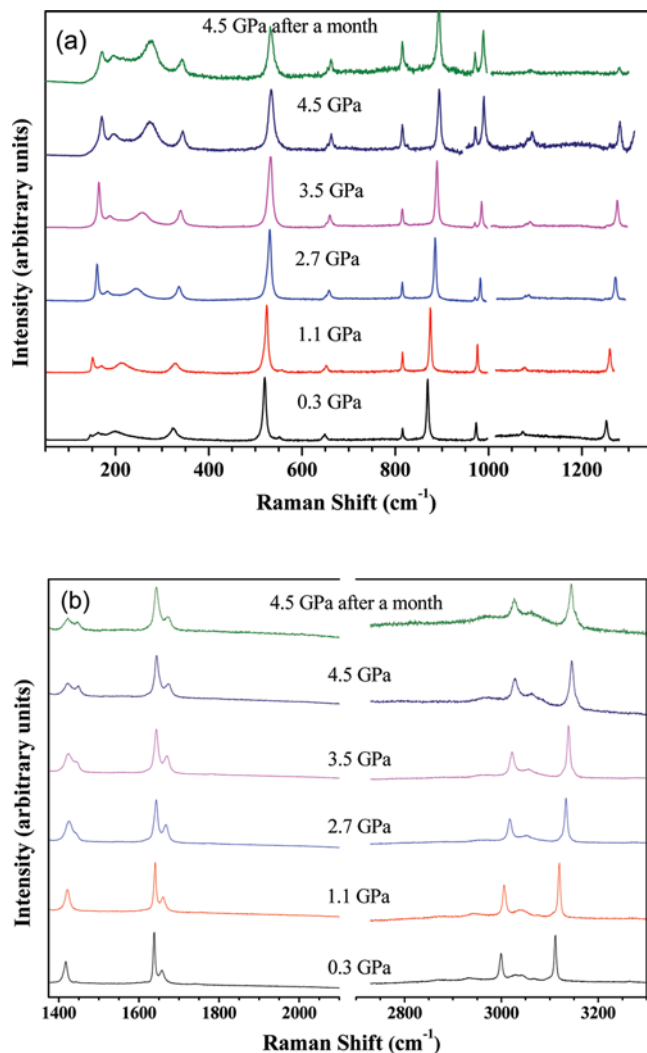


Figure 3. Raman spectra of acrylic acid at selected pressures upon compression in the pressure region of 0.3–4.5 GPa in the spectral region of (a) 100–1300 cm^{-1} and (b) 1400–3300 cm^{-1} .

lectively suggest the phase transition at around 2.7 GPa. We labeled the new phase above 2.7 GPa as phase II, and we provide discussions about the nature of this phase in the next section. Interestingly, the $\tau(\text{C}-\text{C})$ torsional mode at 172 cm^{-1} in the liquid phase at ambient conditions was replaced by a mode at 212 cm^{-1} in the solid phase and was found to exhibit an unusually large pressure-induced stiffening (i.e., 16.8 $\text{cm}^{-1}/\text{GPa}$) compared to all other modes, suggesting that the torsion along the $\text{C}-\text{C}$ bond was increasingly constrained under compression. The pressure was kept nearly constant at 4.5 GPa, and the Raman spectra recorded over a period of a month exhibited no noticeable changes indicating that the high-pressure phase was stable. This observation also suggests slow kinetics for polymerization at this pressure, in contrast to that reported for ethylene.²

B. Raman Spectra in the Pressure Range 3.3–10 GPa.

In another experiment, acrylic acid was pressurized directly to an initial pressure of 3.3 GPa followed by subsequent compression stepwise up to 10 GPa with selected Raman spectra as shown in Figure 5. The Raman spectra at 3.3 GPa were found to be similar to those obtained from the above compression cycle shown in Figure 3 except that upon careful tuning of notch filters, two additional modes were observed in the spectral region of $<200 \text{ cm}^{-1}$ and are most likely associated with lattice vibrations. Similar to phase I, the $\tau(\text{C}-\text{C})$ torsional mode in

phase II continued to stiffen at an even faster rate (i.e., 20 $\text{cm}^{-1}/\text{GPa}$) up to 8 GPa when it merged with the skeletal deformation mode $\delta(\text{C}=\text{C}-\text{C})$ which exhibited significantly less pressure stiffening. The splittings for the $\delta(\text{O}=\text{C}-\text{O})$, $\Omega(\text{C}-\text{H})$, and $\omega(\text{CH}_2)$ modes together with the emergence of the $\nu(\text{CO}_2)_s$ mode were observed in the entire phase II region of 2.7–8 GPa suggesting that there are at least two nonequivalent sets of dimers or molecular clusters in the unit cell via pressure modifications of the phase I structure from the original *s-cis* molecular conformation. More interestingly, although almost all of the Raman modes were found to stiffen monotonically under pressure, the $\delta(\text{CH}_2)$ bending mode (i.e., 1426 cm^{-1} at 2.7 GPa) exhibited a conspicuously soft behavior (i.e., with a negative $d\nu/dP$ of $-3.1 \text{ cm}^{-1}/\text{GPa}$) in the entire phase II region. A soft mode is typically indicative of a later phase transformation if the compression pressure is high enough.²⁰ In this case, the softening of the $\delta(\text{CH}_2)$ bending mode can be regarded as the precursor to the later polymerization during which process the central carbon atom undergoes a gradual transformation from sp^2 to sp^3 hybridization. In-situ high-pressure X-ray or neutron diffraction measurements would be helpful to monitor the changes of bond lengths of acrylic acid as a function of compression to justify the proposed mechanism.

Starting from 6 GPa, pressure-induced broadenings were observed for most of the Raman bands especially in the lattice modes as well as in the $\nu(\text{CH}_2)_s$, $\nu(\text{C}-\text{H})$, and $\nu(\text{CH}_2)_{as}$ modes indicating the onset of a structural disorder, which is another step closer to the final expected polymerization. At 8 GPa, a threshold pressure which also labels the upper bound of phase II of acrylic acid, the Raman spectrum was characterized by extreme band broadening and merging as well as by the dominant depletion of almost all Raman modes of the acrylic acid monomer. Concurrently, a new broad band characteristic of a hydrocarbon-based polymer emerged at 3000 cm^{-1} . These prominent changes suggest that acrylic acid had undergone a transformation to a polymeric phase.

C. Pressure-Induced Polymerization of Acrylic Acid. The successive compression of acrylic acid from 8 to 10 GPa drives the polymeric transition to near completion. At 10 GPa, the Raman spectrum was characterized by weak bands in the 100–2000 cm^{-1} region and by a broad band around 3000 cm^{-1} (Figure 5), completely lacking any characteristics of the acrylic acid monomer, indicating that the polymeric phase was amorphous. To understand the transformation process and its reversibility, we also collected Raman spectra on decompression from 10 GPa to near ambient pressure with the selected spectra shown in Figure 6. As can be seen, acrylic acid remained in the polymeric phase on decompression at pressures above 2.3 GPa. Below 2.3 GPa, some additional bands in the $\text{C}-\text{H}$ stretching region (e.g., 3109, 3040, 2973, 1638, and 852 cm^{-1}) started to be recovered and were most clearly resolved when the sample was completely quenched to ambient pressure. Compared to the ambient-pressure Raman spectrum of acrylic acid before compression, the recovered substance exhibited similar Raman profiles with only minor differences in the CH_2 stretching and in the lattice regions indicating a substantial amount of recovered monomers and thus a partial reversibility of the pressure-induced transformation. Moreover, the observation of the additional CH bands and the missing of one of the $\text{C}=\text{C}$ stretching modes (Figure 6) suggest that the retrieved sample may have complex structures comprising oligomers instead of initial pure monomers.

Polymerization of acrylic acid has been studied previously under various synthetic conditions,¹² and the effect of solvents

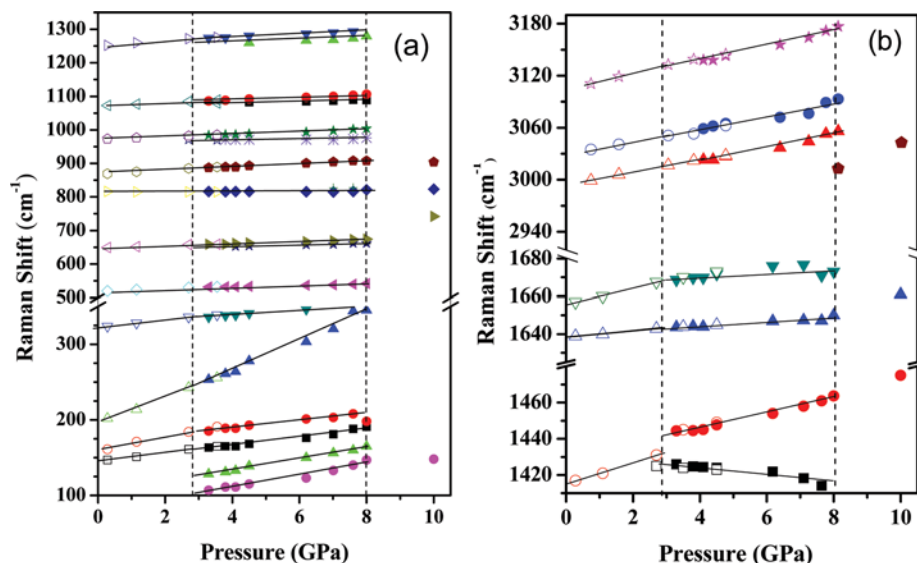


Figure 4. Raman shift of acrylic acid as a function of pressure on compression in the spectral region of (a) 100–1300 cm^{-1} and (b) 1400–3200 cm^{-1} . Open symbols denote data from pressure cycle of 0–4.5 GPa, whereas closed symbols are from pressure cycle of 3.3–10 GPa. Solid straight lines are linear fits to the data. Vertical dashed lines mark the suggested phase-transition boundaries.

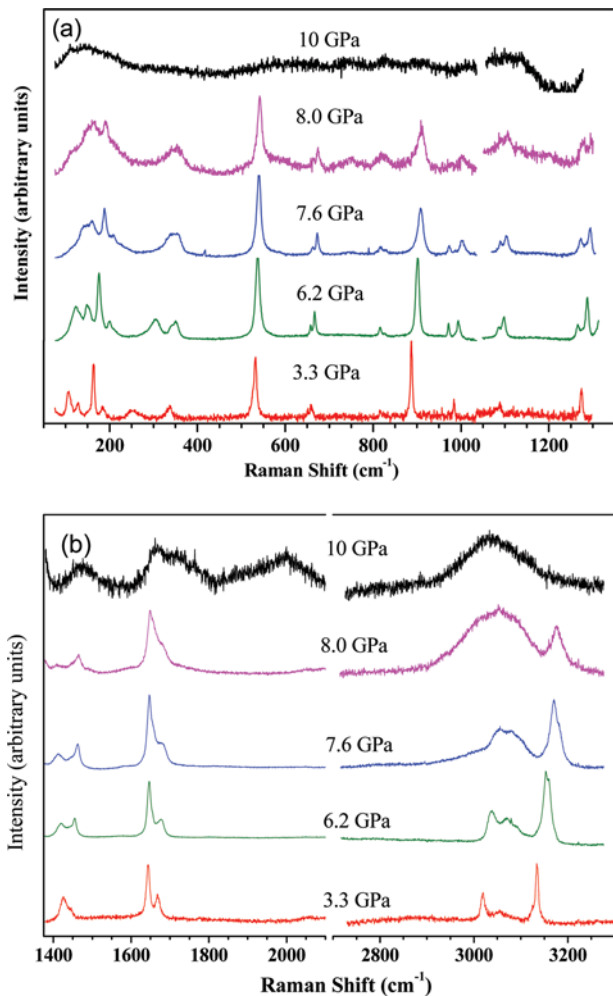


Figure 5. Raman spectra of acrylic acid at selected pressures upon compression in the pressure region of 3.3–10 GPa in the spectral region of (a) 100–1300 cm^{-1} and (b) 1400–3300 cm^{-1} .

on the polymer products has also been reported.^{12,21} It was found that the polymerization of acrylic acid in solutions of various solvents produced three polymer fractions, that is, atactic, syndiotactic, and gel. While the syndiotactic polymer crystallized

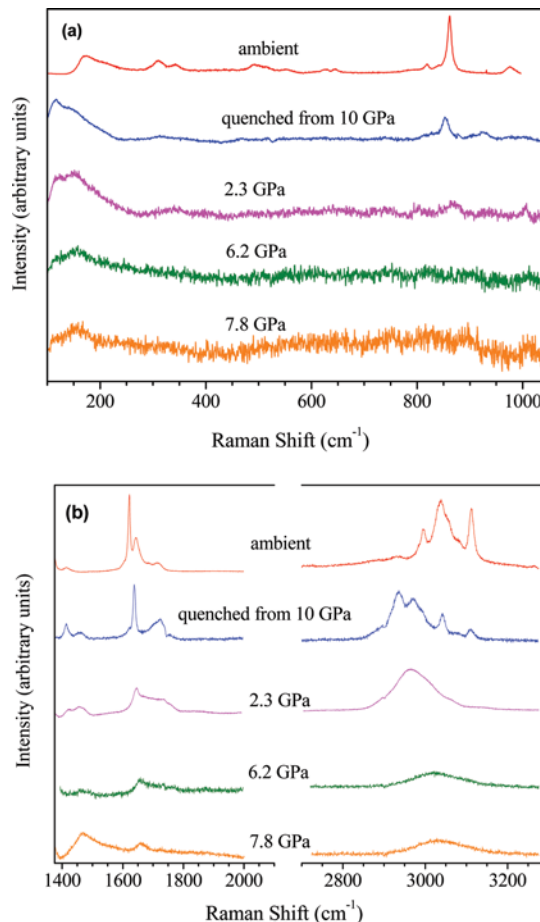


Figure 6. Raman spectra of acrylic acid at selected pressures on decompression in the spectral region of (a) 100–1300 cm^{-1} and (b) 1400–3300 cm^{-1} .

readily, the atactic polymer did not. The gel-type polymer was reported to have a highly entangled structure involving the longest chain of the syndiotactic fraction which is linked by numerous hydrogen bonds.¹² In our study, the pressure-quenched acrylic acid was found to have the gel-like physical appearance.

To further understand the high-pressure structures of the polymeric phase of acrylic acid, we recorded the Raman spectra

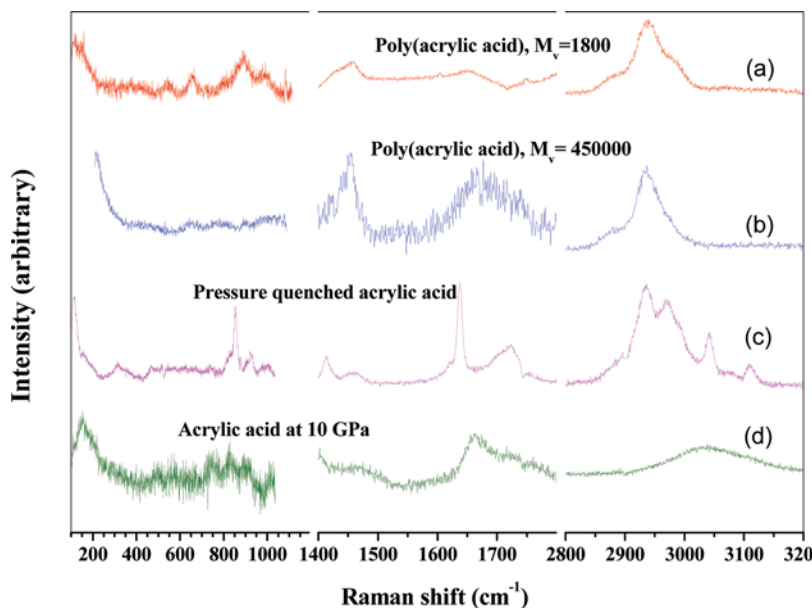


Figure 7. Raman spectrum of poly(acrylic acid) purchased from Aldrich with an average molecular weight of (a) 1800 g/mol and (b) 450 000 g/mol in comparison with that of recovered acrylic acid by decompression from (c) 10 GPa and that of acrylic acid at (d) 10 GPa.

of two commercial poly(acrylic acids) with different average molecular weights (M_v), that is, ~ 1800 and $\sim 450,000$ g/mol, for comparison. The Raman spectra of these polymers are shown in Figure 7 together with those for acrylic acid collected at 10 GPa and upon pressure quenching. Earlier studies attempted to infer the molecular weight and the concentration of poly(acrylic acid) if in solution using the characteristic CH/CH₂ stretching band. However, as shown in Figure 7, the position of this band was found to be nearly the same (i.e., ~ 2938 cm⁻¹) in poly(acrylic acid) of both low and high M_v 's indicating that the peak position of CH/CH₂ band was not sensitive to changes in the molecular weight in this range. Other noticeable differences between the two commercial poly(acrylic acids) include the observation of a broad band at ~ 1664 cm⁻¹ for the high M_v polymer and a few weak bands below 1000 cm⁻¹ (e.g., 503, 612, 824, 923 cm⁻¹) for the polymer of $M_v = 1800$ g/mol. The Raman spectrum of acrylic acid at 10 GPa corresponding to the polymeric phase did not match that of either commercial polymers exactly but apparently exhibited combined spectroscopic activities. For instance, the bands observed at 493, 613, 823, and 902 cm⁻¹ agree with those for low M_v reasonably well, while the broad band at 1662 cm⁻¹ matches that for a high M_v polymer. The CH/CH₂ stretching band at 3035 cm⁻¹ can be regarded as a pressure-shifted band, the frequency of which aligns with that of both polymers when quenched to ambient pressure (Figure 7c). These observations suggest that the polymeric phase likely contains a mixture of polymers with a broader distribution of molecular weights than those of the two commercial polymers examined.

However, the substructures of the pressure-induced polymeric phase might be significantly different than those for both commercial polymers. In addition to the prominent difference in physical appearance (i.e., white solid powders for both commercial polymers vs gel-like pressure-recovered materials), the significant amount of recovered monomers/oligomers evidenced by the observation of the characteristic Raman bands (Figure 7c) suggests that pressure-induced polymerization (or oligomerization) was highly incomplete. Typically, polymerization reactions, either pressure-induced or catalyzed, are irreversible. The partial reversibility of the pressure-induced polymerization of acrylic acid observed in this study can be

interpreted as the result of strong compression-induced association between the monomers and the polymers/oligomers via hydrogen bonding rather than via polymer chain growth. Although acrylic acid is a simple derivative of ethylene, the drastically different pressure behaviors of the two monomers² signified that hydrogen bonding can fundamentally alter the reaction mechanism by "partitioning" the pressure effect from the originally simple unsaturated bonds onto hydrogen bonds.

Finally, since earlier studies by Bini and co-workers have established the important role of photon activation in the pressure-induced polymerization of various monomers,^{2,4-10} it would be of interest to investigate the effect of excitation with different photoenergies on the transition pressures as well as on the nature of the retrieved polymer product of acrylic acid. Furthermore, spectral features involving OH stretching often provide valuable information on the O-H...O hydrogen-bonding interactions. However, the OH stretching mode in acrylic acid was too weak to be observed in the Raman spectra, whereas this mode is usually strong in the infrared absorption spectra. Therefore, in-situ high-pressure infrared absorption studies of this compound would provide further insight into the understanding of polymerizations/oligomerizations and hydrogen-bonding interactions under compression.

5. Conclusions

In summary, we investigated pressure-induced transformations of acrylic acid in a diamond anvil cell up to 10 GPa by Raman spectroscopy. Upon compression, a liquid-to-solid transformation was observed at 0.3 GPa and a solid-to-solid transition was observed at ~ 2.7 GPa with the formation of two new high-pressure crystalline phases, I and II. Phase I has a possibly similar structure to a previously observed low-temperature phase while phase II is a denser phase with strong intermolecular interactions that led to polymerization or oligomerization. At pressures above 8 GPa, acrylic acid was found to transform into a disordered polymeric phase. On release of pressure to ambient, the retrieved polymeric phase was found to contain a substantial amount of acrylic acid monomers or oligomers. Comparative Raman studies on commercial poly(acrylic acid) allowed for the understanding of possible structures of the polymeric phase

of acrylic acid and suggested that hydrogen bonding played a significant role in the pressure-induced polymerization/oligomerization process.

Acknowledgment. This work was supported by a Discovery Grant, a Research Tools and Instruments Grant from the Natural Science and Engineering Research Council of Canada, a Leaders Opportunity Fund from the Canadian Foundation for Innovation, and an Early Researcher Award from the Ontario Ministry of Research and Innovation. C.M. acknowledges the Centre for Chemical Physics (CCP) Fellowship from the University of Western Ontario.

References and Notes

- (1) Schettino, V.; Bini, R. *Phys. Chem. Chem. Phys.* **2003**, *5*, 1951.
- (2) Chelazzi, D.; Ceppatelli, M.; Santoro, M.; Bini, R.; Schettino, V. *Nat. Mater.* **2004**, *3*, 470.
- (3) Bradbury, M.; Hamann, S.; Linton, M. *Aust. J. Chem.* **1970**, *23*, 511.
- (4) Ceppatelli, M.; Santoro, M.; Bini, R.; Schettino, V. *J. Chem. Phys.* **2000**, *113*, 5991.
- (5) Citroni, M.; Ceppatelli, M.; Bini, R.; Schettino, V. *Science* **2002**, *295*, 2058.
- (6) Chelazzi, D.; Ceppatelli, M.; Santoro, M.; Bini, R.; Schettino, V. *J. Phys. Chem. B* **2005**, *109*, 21658.
- (7) Citroni, M.; Ceppatelli, M.; Bini, R.; Schettino, V. *J. Chem. Phys.* **2005**, *123*, 9.
- (8) Citroni, M.; Ceppatelli, M.; Bini, R.; Schettino, V. *J. Phys. Chem. B* **2007**, *111*, 3910.
- (9) Kaminski, K.; Wrzalik, R.; Paluch, M.; Ziolo, J.; Roland, C. M. *J. Phys.: Condens. Matter* **2008**, *20*, 6.
- (10) Schettino, V.; Bini, R.; Ceppatelli, M.; Citroni, M. *Phys. Scr.* **2008**, *78*, 5.
- (11) Xie, S. T.; Song, Y.; Liu, Z. X. *Can. J. Chem.* **2009**, *87*, 1235.
- (12) Chapiro, A.; Dulieu, J. *Eur. Polym. J.* **1977**, *13*, 563.
- (13) Ukaji, T. *Bull. Chem. Soc. Jpn.* **1959**, *32*, 1266.
- (14) Feairheller, W. R.; Katon, J. E. *Spectrochim. Acta, Part A* **1967**, *A23*, 2225.
- (15) Krause, P. F.; Katon, J. E.; Smith, K. K. *Spectrochim. Acta, Part A: Mol. Biomol. Spectrosc.* **1976**, *32*, 957.
- (16) Kulbida, A.; Ramos, M. N.; Rasanen, M.; Nieminen, J.; Schrems, O.; Fausto, R. *J. Chem. Soc., Faraday Trans.* **1995**, *91*, 1571.
- (17) Higgs, M. A.; Sass, R. L. *Acta Crystallogr.* **1963**, *16*, 657.
- (18) Mao, H. K.; Xu, J.; Bell, P. M. *J. Geophys. Res.* **1986**, *91*, 4673.
- (19) Nakabayashi, T.; Kosugi, K.; Nishi, N. *J. Phys. Chem. A* **1999**, *103*, 8595.
- (20) Song, Y.; Liu, Z. X.; Mao, H. K.; Hemley, R. J.; Herschbach, D. R. *J. Chem. Phys.* **2005**, *122*, 174511.
- (21) Yu, J. A.; Liu, H. Z.; Chen, J. Y. *Chin. J. Polym. Sci.* **1999**, *17*, 603.

JP1034757